Penerbit Akademia Baru

Journal of Advanced Research in Micro and Nano Engineering

Journal homepage:
https://www.akademiabaru.com/submit/index.php/armne/index
ISSN: 2756-8210

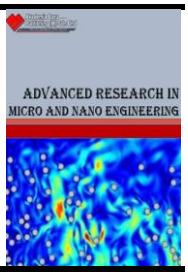

Three-Dimensional Radiative Rotating MHD Nanofluid Flow of Over a Stretched Sheet with Homogeneous-Heterogeneous Chemical Reactions

Swarnalata Jena[1], Kharabela Swain[2], Shaik Mohammed Ibrahim[3], Pandikunta Sreenivasulu[4], Giulio Lorenzini[5,*]

[1] Department of Mathematics, Centurion University of Technology and Management, Bhuaneswar, 752050, India
[2] Department of Mathematics, Gandhi Institute for Technology (GIFT), Bhubaneswar-752054, India
[3] Depa of Engineering Mathematics, College of Engineering, Koneru Lakshmaiah Education Foundation, Vaddeswaram, Andhra Pradesh, 522302, India
[4] Department of Mathematics, Sri Venkateswara College of Engineering, Tirupati-517507, India
[5] Department of Engineering and Architecture, University of Parma, Parco Area delle Scienze 181/A, Parma 43124, Italy

ARTICLE INFO

Article history:
Received 18 April 2024
Received in revised form 20 May 2024
Accepted 25 June 2024
Available online 30 July 2024

Keywords:
MHD; rotating flow; nanofluid; stretching sheet; thermal radiation; heat source

ABSTRACT

CNTs are employed in energy storage, device modelling, automobile parts, water filters, thin-film electronics, coating, and more. The continuous three-dimensional (3D) magnetohydrodynamics (MHD) rotational flow of water-based nanofluid comprising SWCNT and MWCNT past a stretching/shrinking sheet under magnetic field and homogeneous-heterogeneous chemical processes is examined in this study. Heat transport is also examined with thermal radiation and heat source/sink. The governing partial differential equations (PDEs) are transformed to non-linear ODEs using proper similarity transformations and solved numerically using MATLAB's bvp4c package. Graphs and tables show how magnetic field, rotational, suction/injection, thermal radiation, heat source/sink parameters, nanoparticle (NP) volume fraction, and homogeneous and heterogeneous reactions affect velocity, temperature, concentration, skin friction coefficient, and Nusselt number. For larger rotational parameters, the main velocity declines and the second velocity increases, and MWCNTs flow more than SWCNTs.

1. Introduction

Most effective nanoparticles are carbon nanotubes (CNTs), cylindrical structures comprised of one or more graphene (lattice) layers. SWNTs and MWNTs have average sizes of 0.8 to 2 nm and 5 to 20 nm, respectively, despite MWNT diameters exceeding 100 nm. CNT length ranges from 100 nm to 0.5 m. Carbon nanoparticles are used in biosensors, pollutant removal, food, pharmaceutical, gene, and drug delivery safety detection. Also used in gene therapy and tissue regeneration. Whitby and Quirke [1] explored carbon nanotube and nanopipe fluid fluxes. Alessio and Kassinos [2] studied carbon nanotube water density. Jiamei *et al.,* [3] studied carbon nanotube diffusion. Hui *et al.,* [4]

* *Corresponding author.*
E-mail address: giulio.lorenzini@unipr.it

https://doi.org/10.37934/armne.21.1.112126

investigated a water-based carbon nanotube-based hygroresponsive actuator with negative hydrotaxis. Shi *et al.,* [5] studied CTT nanotube water under heat and mass transfer effects. Yacob *et al.,* [6] studied carbon nanotube-rotating flow across a stretching or shrinking sheet. Gul *et al.,* [7] compared CNTs between rotating discs. Kim *et al.,* [8] studied nanoreactor-based graphene nanoribbon edge vibration. Many recent studies focused on fluid flows due to revolving discs. Due to its many applications in rotating equipment, computer storage devices, thermal power producing systems, aeronautical science, and air. Power law fluid flow over a revolving disc was shown by Anderson *et al.,* [9]. Nazar *et al.,* [10] studied fluid rotation over stretched surfaces. Sharma [11] examined the rheological impact of forced convection ferrofluid past rotating disc. Slanted stagnation point flow across a revolving disc was examined by Sankar and Sahoo [12]. Farooq *et al.,* [13] studied water-based Ferro nanofluid axisymmetric flow past a rotating disc. Carreau fluid past a spinning disc was studied by Ming *et al.,* [14].

Amplification of sun and star behaviour is possible with magneto hydrodynamic flow. The solar corona structure is well described by MHD. The ability of MHD to spin the magnetic field, which causes fluid currents. MHD is used in blood pumps and plasma equipment. Electromagnetic forces pump liquid sodium to cool nuclear fission reactors. MHD flow of spinning electrically conducting fluids in a magnetic field is used in many geophysics and astronomy applications. Gholinia *et al.,*[15] discussed MHD's effect on Ering-Powell fluid past a rotating disc. The Cattaneo-Christov effect on inclined MHD micropolar fluid over a stretchable spinning disc was studied by Doh *et al.,* [16]. The effects of Navier slip and aligned MHD on carbon nanotube free convective radiative flow were discussed by Sreenivasulu *et al.,* [17]. Sharma *et al.,* [18] studied MHD boundary layer flow over a porous rotating disc. Swain *et al.,* [19] examined how homogeneous and heterogeneous chemical reactions and exponential heat sources affect nanofluid MHD flow past an elongating sheet. Thermal boundary conditions affected the 3D MHD rotating flow of nanofluids via an elongating sheet, according to Mishra *et al.,* [20]. Many studies studied MHD's effect on inclined or non-inclined flow across a spinning disc [21-25].

Surfaces emit electromagnetic radiation in all directions as thermal radiation. Radiation is crucial in high-temperature and space technology. Polymer industry heat transport is largely controlled by radiation. Surface thermal radiations are important due to the convective heat transfer coefficient. Radiation affected Maxwell nanofluid past a stretched porous rotating disc, according to Zhou *et al.,* [26]. Hussain *et al.,* [27] examined MHD and non-linear radiation on 3D rotational nanofluid across a stretchable surface. Bashir *et al.,* [28] described thermophoresis' effect on radiative flow past a porous spinning disc. Shama [29] studied radiation and dissipation on FHD flow past a porous spinning disc. Recently, Sobia *et al.,* [30] explained radiation and Cattaneo-Christov heat flow on ternary hybrid nanofluid between double rotating discs. Arif *et al.,* [31] studied tri-hybrid nanofluid viscoelastic radiative flow past a spinning disc. Swain *et al.,* [32] recently examined radiation's effect on 3D Maxwell nanofluid beyond a permeable stretching sheet. Nagalakshmi *et al.,* [33] modelled Williamson Nanofluid flow using hybrid carbon nanotubes for 3D entropy creation over a stretched sheet.

Biochemical, catalytic, and combustion systems use homogeneous and heterogeneous reactions. Chemical reactions are homogeneous or heterogeneous depending on whether they occur in fluid or on catalytic surfaces. The interaction between homogeneous and heterogeneous reactions that create and consume reactant species at various rates in the fluid and on catalytic surfaces is usually complicated. Chaudhary and Merkin [34] published a simple isothermal model for homogeneous and heterogeneous processes. Nandkeolyar *et al.,* [35] examined chemical reaction and transverse magnetic field effects on stretching sheets. Renuka *et al.,* [36] showed homogeneous-heterogeneous interactions between stretchy rotating discs. Al-Kouz *et al.,* [37] explored homogeneous and

heterogeneous chemical reactions on hybrid nanofluid with an aligned magnetic field and exponential space-based heat source. Sadiq and Hayat [38] examined how chemical reaction affects Reiner-Rivlin nanofluid Entropy optimise flow past a rotating disc. Kumar and Sharma [39] studied Stefan blowing's effect on Reiner-Rivlin fluid flow past a revolving disc. Nanofluid flow over stretching/shrinking sheets has been studied by several researchers using a variety of theoretical approaches [40-46].

The authors believe no research has considered thermal radiation and heat source impacts on 3D MHD rotational flow of nanofluids across a stretching sheet with homogeneous-heterogeneous chemical processes. This work uses water as the base fluid and SWCNT and MWCNT as nanoparticles. The current study is motivated by: It is generally known that boundary layer flow separates in negative pressure gradients. Stretching the plate, rotating the fluid mass about its axis, diffusing carbon nanoparticles (SWCNT and MWCNT), and homogeneous-heterogeneous chemical reactions that involve both the flowing fluid and the solid boundary's heat and mass transfer properties complicate boundary layer flow. So, the upcoming research is a real-world boundary value problem that involves numerical skill and intelligence. The solution has intriguing results, as stated in the findings and discussion.

Below are the research questions:

- What impact does the electromagnetic force have on nanofluid and nanoparticle flow through a stretching/shrinking sheet?
- How does rotating fluid mass about the z-axis impact three-dimensional problems?
- What impact does the heat source/sink have on the thermal boundary layer?
- How do homogeneous and heterogeneous reactions affect species concentration?

2. Formulation of the Problem

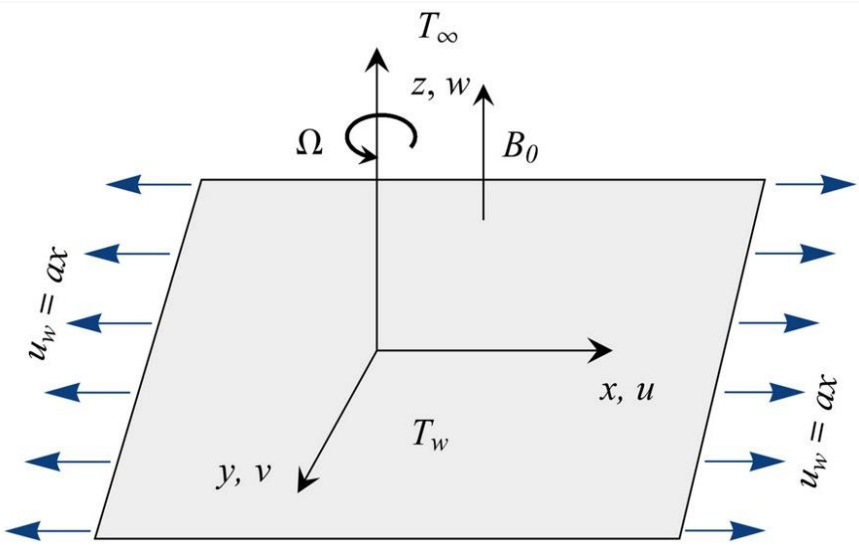

Fig. 1. Flow geometry

Consider a steady 3D rotating flow of water and kerosene based nanofluids containing SWCNT and MWCNT as nanoparticles past a stretching/shrinking sheet in the existence of a magnetic field, homogeneous and heterogeneous chemical reaction. Further, the heat transfer phenomena is analysed in the presence of thermal radiation and heat source/sink. The flow is caused by the stretching of the sheet at $z = 0$ along the *x*-axis with rate $u_w = ax$. The fluid is rotating at an angular

velocity Ω in the z-direction. The transverse magnetic field of strength B_0 is applied perpendicular to the sheet (see Figure 1). Let T_w and T_∞ be the temperatures on the surface of the sheet and ambient state. It is also supposed that a simple homogeneous-heterogeneous reaction model exists between the species *A* and *B* as proposed by Chaudhary and Merkin [34] in the following form

$$A + 2B \to 3B, \text{ rate} = k^* c_1 c_2^2, \tag{1}$$

Whereas, a heterogeneous first order, the isothermal reaction takes place on the catalyst surface, as

$$A \to B, \text{ rate} = h_s c_1 \tag{2}$$

Where k^* and h_s are the rate constants. We assume that both reaction processes are isothermal.

The governing equations and corresponding boundary conditions following Yacob *et al.,* [6] are given by

$$u_x + v_y + w_z = 0, \tag{3}$$

$$uu_x + vu_y + wu_z = 2\Omega v + \nu_{nf}\, u_{zz} - \frac{\sigma_{nf}}{\rho_{nf}} B_0^2 u, \tag{4}$$

$$uv_x + vv_y + wv_z = -2\Omega u + \nu_{nf}\, v_{zz} - \frac{\sigma_{nf}}{\rho_{nf}} B_0^2 v, \tag{5}$$

$$\left(\rho c_p\right)_{nf}\left(uT_x + vT_y + wT_z\right) = \left(k_{nf} + \frac{16\sigma^* T_\infty^3}{3k^*}\right) T_{zz} + Q^*\left(T - T_\infty\right), \tag{6}$$

$$u\, c_{1_x} + v\, c_{1_y} + w c_{1z} = D_A\, c_{1_{zz}} - k^* c_1 c_2^2 \tag{7}$$

$$u\, c_{2_x} + v\, c_{2_y} + w c_{2_z} = D_B\, c_{2_{zz}} - k^* c_1 c_2^2 \tag{8}$$

$$u = \delta u_w = \delta a x, v = v_w = 0, w = -w_0, T = T_w, D_A c_{1_z} = h_s c_1, D_B c_{2_z} = -h_s c_1 \text{ at } z = 0, \tag{9}$$

$$u \to 0, v \to 0, T \to T_\infty, C_1 \to C_0, C_2 \to 0 \text{ as } z \to \infty. \tag{10}$$

Where σ^* is the Stefan-Boltzmann constant, k^*, the mean absorption coefficient, w_0 is the constant mass flux with $w_0 > 0$ indicates injection, while $w_0 < 0$ is for suction. Further, δ is the stretching or shrinking parameter with $\delta > 0$ for stretching, $\delta < 0$ for shrinking and $\delta = 0$ for the static surface.

Using the following similarity transformations (see ref. [34])

$$\eta = z\sqrt{\frac{a}{\nu_f}}, u = axf'(\eta), v = axg'(\eta), w = -\sqrt{a\nu_f}\, f(\eta),$$
$$\theta(\eta) = \frac{T - T_\infty}{T_w - T_\infty}, C_1 = a_0\Phi(\eta), C_2 = a_0 h(\eta) \tag{11}$$

The Eq. (3) – (10) become,

$$f''' = (\lambda_1\lambda_2)^{-1}\left(f'^2 - ff'' - 2\gamma g + \gamma\lambda_2\lambda_3 M f'\right), \tag{12}$$

$$g'' = (\lambda_1\lambda_2)^{-1}\left(f'g - fg' - 2\gamma f' + \gamma\lambda_2\lambda_3 M g\right), \tag{13}$$

$$\theta'' = -\frac{\Pr}{\lambda_4}\left(\frac{k_{nf}}{k_f} + \frac{4}{3}R\right)^{-1}\left(f\theta' + Q\theta\right) \tag{14}$$

$$\Phi'' = -Sc\left(f\Phi' - k_c\Phi h^2\right) \tag{15}$$

$$h'' = -Sc\xi^{-1}\left(fh' + k_c\Phi h^2\right) \tag{16}$$

$$f(0) = 0,\ f'(0) = \delta, g(0) = 0, \theta(0) = 1, \Phi'(0) = k_c\Phi(0), \tag{17}$$

$$f'(\infty) \to 0, g(\infty) \to 0, \theta(\infty) \to 0, \Phi(\infty) \to 1, h(\infty) \to 0. \tag{18}$$

(where k_c, measure of the strength of heterogeneous reaction).

Assuming the equal diffusivity of chemical species *A* and *B* i.e. $\xi = 1$ (see ref. [19,36,37]), we have

$$\Phi(\eta) + h(\eta) = 1 \tag{19}$$

Using Eq. (19), the Eq. (15) and (16) reduce to

$$\Phi'' = -Sc\left\{f\Phi' - k_c\Phi(1-\Phi)^2\right\}, \tag{20}$$

Also, the corresponding boundary conditions are reduced to

$$\Phi'(0) = k_c\Phi(0), \Phi(\infty) \to 1 \tag{21}$$

where $\gamma = \frac{\Omega}{a}, \lambda_1 = (1-\phi)^{-2.5}, \lambda_2 = \left[(1-\phi) + \phi\left(\frac{\rho_s}{\rho_f}\right)\right]^{-1}, \lambda_3 = 1 + \frac{3(\sigma_s - \sigma_f)\phi}{(\sigma_s + 2\sigma_f) - (\sigma_s - \sigma_f)\phi'}$

$$\lambda_4 = \left[(1-\phi) + \frac{(\rho c_p)_s}{(\rho c_p)_f}\phi \right]^{-1}, k_s = \frac{h_s}{D_A}\sqrt{\frac{\nu_f}{a}}, M = \frac{\sigma_f B_0^2}{\rho_f \Omega}, R = \frac{4\sigma^* T_\infty^3}{k_f k^*}, \Pr = \frac{\nu_f (\rho c_p)_f}{k_f},$$

$$Q = \frac{Q^*}{a(\rho c_p)_f}, \xi = \frac{D_A}{D_B}, Sc = \frac{\nu_f}{D_A}, k_c = \frac{k^* a_0^2}{a}.$$

The thermo-physical properties such as density, viscosity, heat capacity and thermal conductivity of nanofluid are given in Table 1. Further, the thermophysical properties of water and nanoparticles are given in Table 2.

2.1 Physical Quantities of Engineering Interest

The force coefficients (C_{fx}, C_{fy}) and local Nusselt number (Nu_x) are defined as

$$C_{fx} = \frac{\mu_{nf}}{\rho_f u_w^2}\frac{\partial u}{\partial z}\bigg|_{z=0} \Rightarrow C_{fx}\sqrt{\mathrm{Re}_x} = (1-\phi)^{-2.5} f''(0), \tag{22}$$

$$C_{fy} = \frac{\mu_{nf}}{\rho_f u_w^2}\frac{\partial v}{\partial z}\bigg|_{z=0} \Rightarrow C_{fy}\sqrt{\mathrm{Re}_x} = (1-\phi)^{-2.5} g'(0), \tag{23}$$

$$Nu_x = -\frac{x k_{nf}}{k_f (T_w - T_\infty)}\frac{\partial T}{\partial z}\bigg|_{z=0} \Rightarrow \frac{Nu_x}{\sqrt{\mathrm{Re}_x}} = -\left(\frac{k_{nf}}{k_f} + \frac{4}{3}R\right)\theta'(0), \tag{24}$$

where $\mathrm{Re}_x = \frac{u_w x}{\nu_f}$ is the Reynolds number.

Table 1
Effective nanofluid properties [32]

Density	$\rho_{nf} = (1-\phi)\rho_f + \phi\rho_s$
Viscosity	$\mu_{nf} = (1-\phi)^{-2.5}\mu_f$
Heat capacity	$(\rho c_p)_{nf} = (1-\phi)(\rho c_p)_f + \phi(\rho c_p)_s$
Thermal conductivity	$\frac{k_{nf}}{k_f} = \frac{2k_f + k_s - 2\phi(k_f - k_s)}{2k_f + k_s + \phi(k_f - k_s)}$
Electrical conductivity	$\sigma_{nf} = \sigma_f\left[1 + \frac{3\phi(\sigma_s/\sigma f - 1)}{\sigma_s/\sigma f - 2 - (\sigma_s/\sigma f - 1)\phi}\right]$

Table 2
Thermophysical properties of H_2O, Cu and TiO_2 [17]

Physical property	H_2O	SWCNT	MWCNT
$\rho\left(kg/m^3\right)$	997.1	2600	1600
$c_p\left(J/KgK\right)$	4180	425	796
$k\left(W/mK\right)$	0.6071	6600	3000
$\sigma\left(\Omega^{-1}m^{-1}\right)$	0.05	4.8×10^7	3.3×10^6

Table 3
Comparison of results with existing literatures when $\phi = M = R = Q = k_c = 0$

γ	Nazar *et al.,* [10]		Hussain *et al.,* [27]		Mishra *et al.,* [20]		Present study	
0	-1	0	-1	0	-1	0	-1.000062	0
0.5	-1.1384	-0.5128	-1.1384	-0.5128	-1.13837	-0.51276	-1.138374	-0.512760
1.0	-1.3250	-0.8371	-1.3250	-0.8371	-1.32502	-0.83709	-1.325028	-0.837097
2.0	-1.6523	-1.2873	-1.6523	-1.2873	-1.65235	-1.28726	-1.652352	-1.287258

3. Methodology

3.1. Numerical Analysis

The Runge-Kutta fourth order approach and shooting technique are used to solve the nonlinear ODEs (12), (14) and (20) numerically with the required boundary conditions (17), (18), and (21). Bvp4c in MATLAB conducts the solution procedure. The solution has intriguing outcomes, as described in the findings and discussion. In a transverse magnetic field, this also bridges electrically nonconducting and conducting flow. This approach reduces the governing equations to first-order differential equations. A computation with an initial mesh and a guess for solution values at mesh points must specify boundary condition guess values. To improve accuracy, self-correction is performed.

3.2. Validation of the Study

To confirm the code, we obtain the results for the skin friction coefficient when $\phi = M = R = Q = k_c = 0$ for various values of γ which are shown in Table 3. These outcomes are found in good agreement with the results reported by Nazar *et al.,* [10], Hussain *et al.,* [27], and Mishra *et al.,* [20].

Table 4
Numerical values of skin friction coefficients for $\Pr = 6.2.$

M	δ	γ	ϕ	SWCNT-water		MWCNT-water	
				$f''(0)$	$g'(0)$	$f''(0)$	$g'(0)$
0.1	0.5	0.1	0.01	-0.369817	-0.083489	-0.371695	-0.083903
0.5				-0.382311	-0.079428	-0.384371	-0.079783
1.0				-0.397625	-0.075042	-0.399908	-0.075338
	1.0			-1.061734	-0.115941	-1.067485	-0.116441
	1.5			-1.913576	-0.146453	-1.923686	-0.147110
	0			0	0	0	0
	-0.5			-0.227739	0.898060	-0.228995	0.901598
	-0.8			-0.575541	3.403416	-0.578729	3.419571

	-1.0			-0.833488	6.142418	-0.838025	6.172188
	1.0	0.5		-1.312439	-0.430608	-1.320650	-0.432056
		1.0		-1.588544	-0.682885	-1.599056	-0.684990
		2.0		-2.037970	-1.032574	-2.051993	-1.035580
		-0.5		-0.985802	0.633149	-0.989241	0.637614
		-1.0		-1.105762	1.054124	-1.109263	1.061690
		1.0	0.05	-1.637198	-0.689869	-1.690582	-0.699750
			0.1	-1.710738	-0.702165	-1.820488	-0.720500
			0.2	-1.908999	-0.739084	-2.147472	-0.770976

Table 5
Numerical values of Nusselt number when $\delta = M = 0.5$ and $\Pr = 6.2.$

ϕ	γ	δ	Q	R	$-\theta'(0)$	
					SWCNT-water	MWCNT-water
0.01	0.1	0.5	0.1	0.1	1.0342644	1.0329818
0.05					1.0772132	1.0709307
0.1					1.1313735	1.1191899
0.2					1.2424881	1.2200340
	0.5				1.0825595	1.0298784
	1.0				0.8486581	0.7331277
	1.5				0.5109763	0.2250330
	0.1	1			2.0195617	1.9998053
		1.5			2.5716963	2.5512781
		0			0.5102789	0.4870901
		-0.5			-0.6137176	-0.6141259
		-1			-0.3965665	-0.3965981
		0.5	0.2		0.8294231	0.7852637
			0.3		0.2446973	0.1356846
			0		1.5720091	1.5600178
			-0.1		1.8516770	1.8458683
			-0.2		2.0978923	2.0962389
			0.1	0.3	1.3046514	1.2778626
				0.5	1.3599534	1.3286406
				1.0	1.4743859	1.4310499

4. Results and Discussion

4.1 Analysis of Results

Analysis of graphed results: The velocity profiles decrease monotonically with space variable and reach potential far off the bounding surface. About the main velocity. However, the secondary velocity's quick surge and decrease indicate flow instability. Metallic and metallic oxide nanoparticles have opposite primary and secondary velocity responses. Magnetic parameter decreases primary velocity but increases secondary velocity beyond surface layers. In addition, the magnetic parameter raises flow domain temperature. Increased rotational parameters lower primary velocity for both nanofluids. Secondary velocity rises with rotation. Nanoparticle volume fraction affects temperature in an intriguing way. Without nanoparticles, temperature is higher on the boundary but lower for non-zero volume fractions. This shows that nanoparticles cool the border. This helps cool electronics, reactors, etc. The effect of the Biot number is interesting because metallic nanofluid generates heat whereas metallic oxide absorbs heat. This affects electronic device heating/cooling when needed. Also, the heat source raises the nanofluid temperature while the sink lowers it.

4.2 Discussion of Results

Following discussion reveals the effect of characterizing parameters, particularly, those parameters which account for the novelties of the present study such as the heat source parameter (Q) measuring the thermal power per unit volume, thermal radiation parameter (R) that contributes to the transfer of thermal energy, nano fluid volume fraction ϕ and homogeneous k_c - heterogeneous chemical reactions. The flow analysis brings to its fold the effect of body forces like electromagnetic force *(M)* and rotational force (γ) due to the rotating frame of reference.

The impact of electromagnetic force (*M*) on axial velocity and transverse velocity are depicted in Figures 2 and 3 respectively. The magnetic parameter *M* is the ratio of electromagnetic force to viscous force, it acts as a Lorentz, so the larger values of M reduce the viscosity of the fluid due to this fact the axial velocity of the fluid increases with an increase in the electromagnetic force. Also, it is noticed that the velocity converges faster in *MWCNT* than the *SWCNT*. The opposite behavior is noticed in the case of the transverse velocity of the fluid.

The axial and transverse velocity profiles for different values of stretching parameters (δ) are shown in Figures 4 and 5 respectively. Since $\delta > 0$ for stretching, $\delta < 0$ for shrinking and $\delta = 0$ for the static surface. From Figure 3 it is noticed that the axial velocity of the nanofluid *(SWCNT)* decreases in the stretching case and increases in the shrinking case. Also, it is evident that the transverse velocity of the fluid decreases near the surface and increases away from the surface in stretching cases while it shows the opposite behavior in the shrinking case.

Figures 6 and 7 describe the role of rotational parameters γ on the velocity components. The radial velocity (Figure 6) of the nanofluid decreases with an increase in the value of the rotational parameter and the azimuthal velocity decreases near the surface and increases away from the surface (Figure 7), due to the fact that γ defines the ratio of the swirl rate to the stretch rate and it gives us a measure of the swirl rate to the stretch rate. The temperature of the nanofluid increases with an increase in the rotational parameter (Figure 8) and it is noticed that the impact of *MWCNT* is more than the *SWCNT*.

Thermal radiation impact on temperature is shown in Figure 9. The temperature of the nanofluid increases with increases in the radiation parameter *R*. Also it is noticed that the temperature in *SWCNT* is larger than the general base fluid, due to the nanofluids having more thermal conductibility than the base fluid.

The effect of the heat source or sink parameter on the temperature of the nanofluid is depicted in Figure 10. The temperature of the nanofluid increases with an increase in heat source or sink parameter *(Q)*. Also, it is noticed that the temperature of *SWCNTs* is higher than the temperature in the general case. Since with an increase in the heat source parameter, the nanofluid becomes warmer by this means adding to the temperature of the nanofluid.

Figures 11 and 12 show the variations in the homogeneous and heterogeneous reactions over the concentration profiles. The concentration of the nanofluid reduces with the larger values of homogeneous reaction which is shown in Figure 11. Also, it is noticed that the *SWCNT* produces higher values than the original fluid. The same behavior is noticed in heterogeneous case (Figure 12). The base fluid and the nanotubes are in the same stage in the homogeneous reaction and in case of heterogeneous reaction.

The impact of Schmidt number *Sc* on the concentration profile is shown in Figure 13. Since the Schmidt number defines the ratio of viscosity and mass diffusivity. It is observed that the greater

Schmidt number results in the enhancement in the concentration of the nanofluid, due to an increase in the Schmidt number leading to decreases in the mass diffusivity of the fluid. Also, it is noticed that the concentration is high for higher values of the rotation parameter.

The influence of engineering quantities such as $f''(0), g'(0)$ and $-\theta'(0)$ for various physical parameters for different carbon nanotubes such as *SWCNTs* and *MWCNTs* with water based nonofluid is shown in tables 4 and 5. Table 4 displayed the variations of the surface skin friction along the axial direction as well as the transverse directions for various physical parameters such as magnetic parameter *(M)*, Stretching/ shrinking ratio parameter (δ), rotational parameter (γ) and nanotube volume fraction (ϕ). From this table, it is noticed that, As the rise in magnetic parameter results the velocity gradient in the axial direction $(f''(0))$ decreases in both *SWCNTs* and *MWCNTs* and the opposite behavior is noticed in the transverse velocity gradient $(g'(0))$. Also, it is noticed that the velocity gradient decreases with an increase in stretching parameter increases while the stretching parameter decreases results the axial velocity gradient decreases and the transverse velocity gradient increases. The same behavior is observed in the case of the rotational parameter. It is depicted in the table that the velocity gradient decreases with an increase in the volume fraction parameter. The temperature gradient for various physical parameters is depicted in Table 5. It is evident that the temperature gradient increases for higher values of the volume fraction parameter or radiation parameter or stretching/shrinking parameter while the opposite behavior is noticed in the case of the rotational parameter. The temperature gradient falls down in the stretching case and rises in the shrinking case.

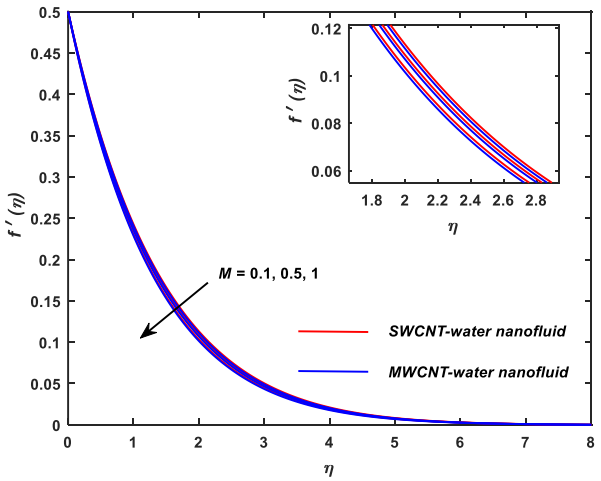

Fig. 2. Axial velocity profile versus *M*

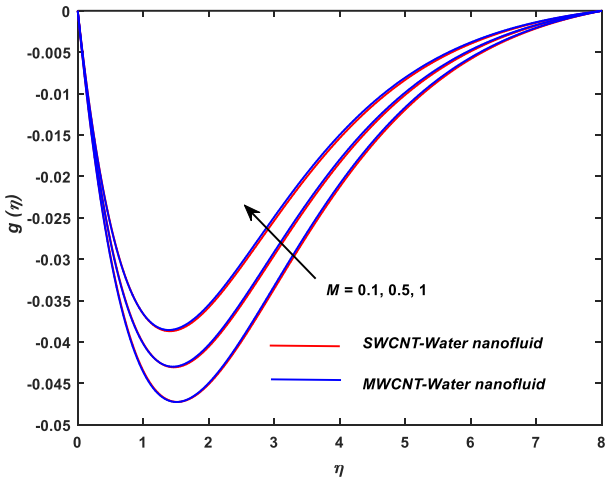

Fig. 3. Transverse velocity profile versus *M*

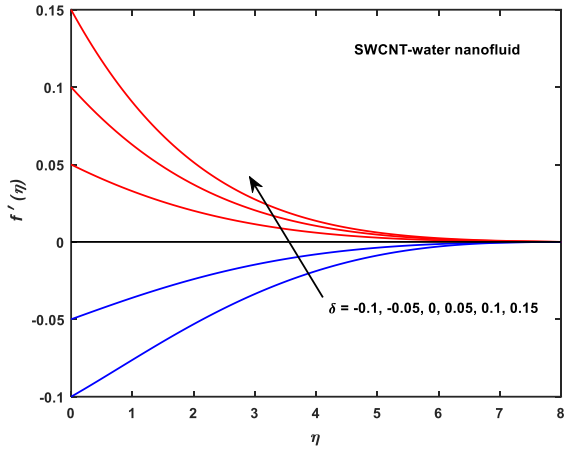

Fig. 4. Axial velocity profile versus δ

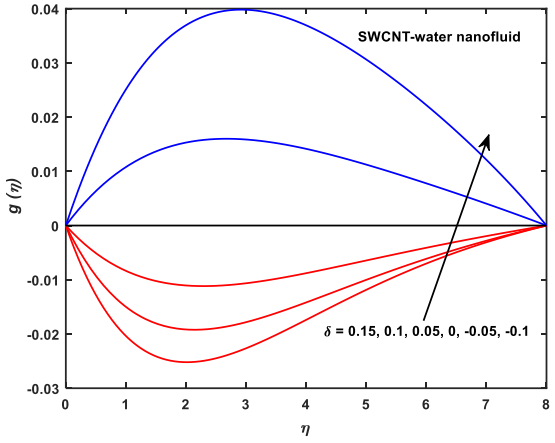

Fig. 5. Transverse velocity profile versus δ

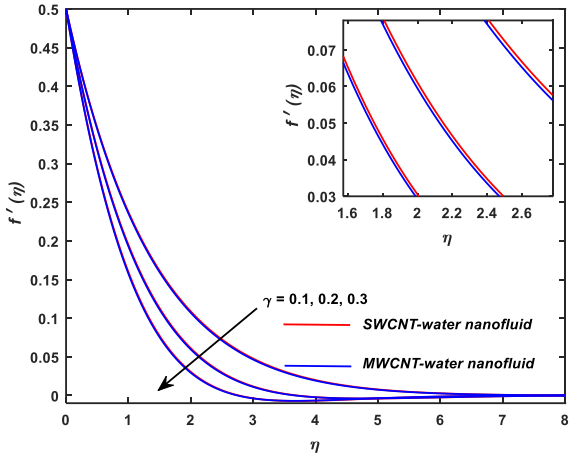

Fig. 6. Axial velocity profile versus γ

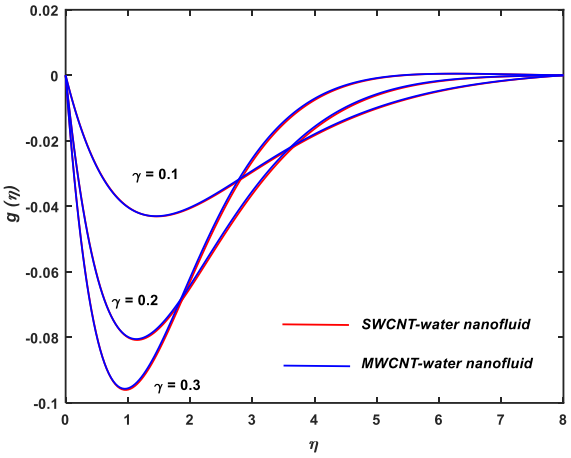

Fig. 7. Transverse velocity profile versus γ

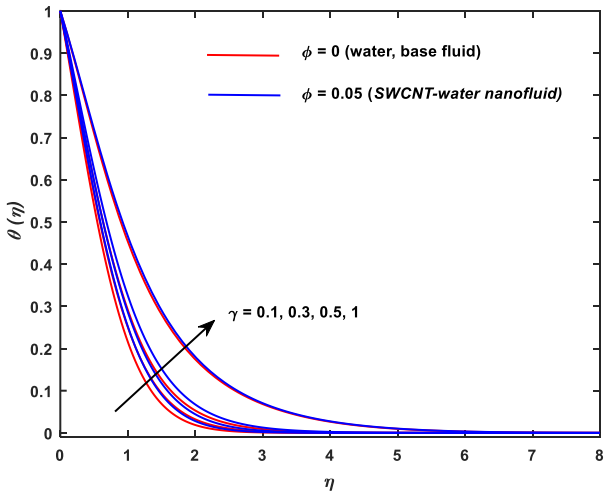

Fig. 8. Temperature profile versus γ

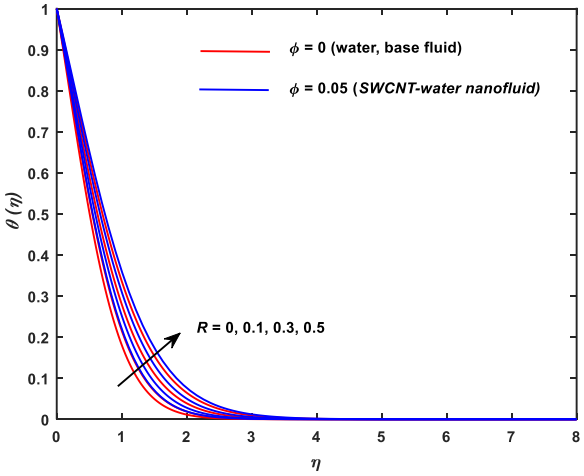

Fig. 9. Temperature profile versus *R*

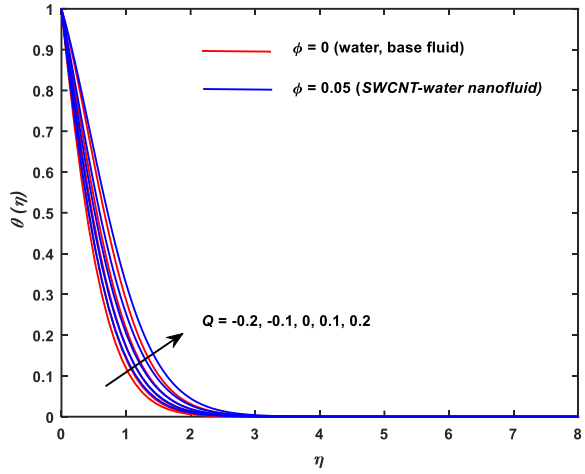

Fig. 10. Temperature profile versus Q

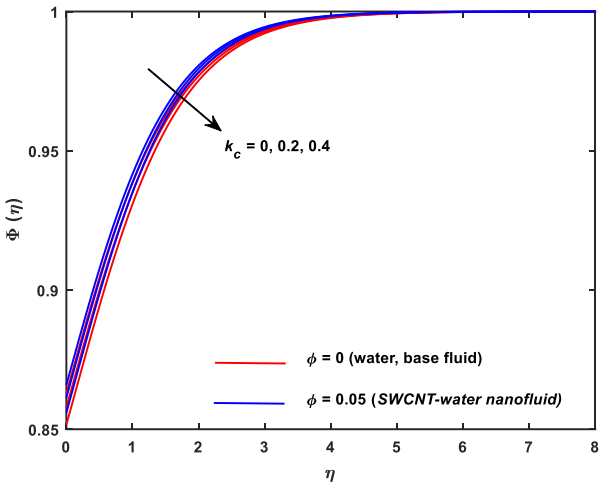

Fig. 11. Concentration profile versus k_c

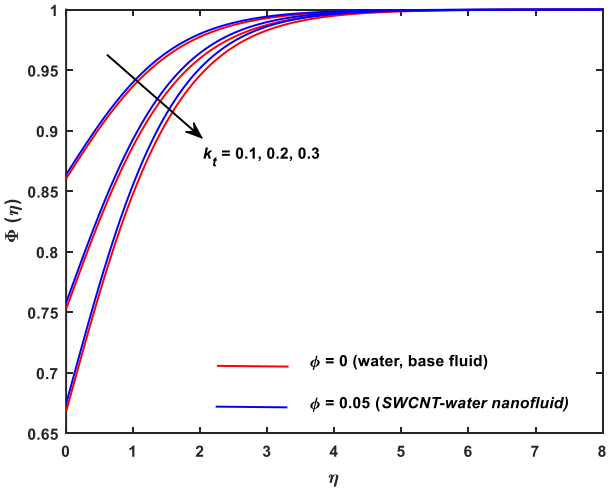

Fig. 12. Concentration profile versus k_t

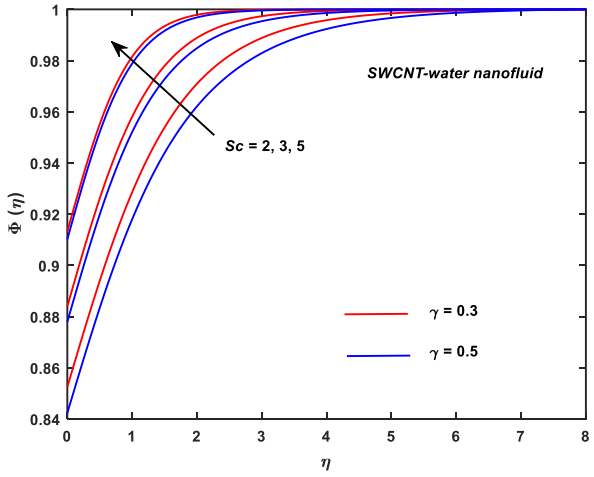

Fig. 13. Concentration profile versus Sc

5. Conclusions

A 3D MHD rotating flow of nanofluids across a stretching sheet with homogeneous-heterogeneous chemical processes is investigated in this work, taking thermal radiation and heat source into account. Physical aspects are discussed using graphs and tables, followed by some key findings:

i. The velocity profiles decrease monotonically with space variables and reach potential conditions far from the bounding surface.
ii. Magnetic parameters diminish primary velocity but boost secondary velocity after specific layers near the surface.
iii. As the rotational parameter increases, primary velocity drops for both nanofluids, but secondary velocity increases.
iv. Nanoparticles cool the border by lowering its temperature.
v. Heat source raises nanofluid temperature, whereas sink lowers it.

Reference

[1] Whitby, M., and N. Quirke. "Fluid flow in carbon nanotubes and nanopipes." *Nature nanotechnology* 2, no. 2 (2007): 87. https://doi.org/10.1038/nnano.2006.175

[2] Alexiadis, Alessio, and Stavros Kassinos. "The density of water in carbon nanotubes." *Chemical Engineering Science* 63, no. 8 (2008): 2047-2056. https://doi.org/10.1016/j.ces.2007.12.035

[3] Feng, Jiamei, Peirong Chen, Dongqin Zheng, and Weirong Zhong. "Transport diffusion in deformed carbon nanotubes." *Physica A: Statistical Mechanics and its Applications* 493 (2018): 155-161. https://doi.org/10.1016/j.physa.2017.10.014

[4] Chen, Hui, Yuanhang Ge, Sunjie Ye, Zhifeng Zhu, Yingfeng Tu, Denteng Ge, Zhao Xu, Wei Chen, and Xiaoming Yang. "Water transport facilitated by carbon nanotubes enables a hygroresponsive actuator with negative hydrotaxis." *Nanoscale* 12, no. 10 (2020): 6104-6110. https://doi.org/10.1039/D0NR00932F

[5] Cai, Kun, Xin Zhou, Jiao Shi, and Qing-Hua Qin. "Water transport behaviors in a CTT-type nanotube system." *Microfluidics and Nanofluidics* 26, no. 11 (2022): 91. https://doi.org/10.1007/s10404-022-02598-0

[6] Yacob, Nor Azizah, Nor Fadhilah Dzulkifli, Siti Nur Alwani Salleh, Anuar Ishak, and Ioan Pop. "Rotating flow in a nanofluid with CNT nanoparticles over a stretching/shrinking surface." *Mathematics* 10, no. 1 (2021): 7. https://doi.org/10.3390/math10010007

[7] Khan, Saad A., Imran Khan, Taza Gul, Imran Ullah, Mujeeb ur Rehman, Asif Ullah, and Said Anwar Shah. "Comparative analysis of the CNTs nano fluid flow between the two gyrating disks." *Advances in Mechanical Engineering* 14, no. 4 (2022): 16878132221093124. https://doi.org/10.1177/16878132221093124

[8] Kwon, Oh Kuen, Jae-Moon Kim, Hag-Wone Kim, Ki-Sub Kim, and Jeong Won Kang. "A study on nanosensor based on graphene nanoflake transport on graphene nanoribbon using edge vibration." *Journal of Electrical Engineering & Technology* 18, no. 1 (2023): 663-668. https://doi.org/10.1007/s42835-022-01302-0

[9] Andersson, H. I., E. De Korte, and R. Meland. "Flow of a power-law fluid over a rotating disk revisited." *Fluid dynamics research* 28, no. 2 (2001): 75. https://doi.org/10.1016/S0169-5983(00)00018-6

[10] Nazar, R., N. Amin, and I. Pop. "Unsteady boundary layer flow due to a stretching surface in a rotating fluid." *Mechanics Research Communications* 31, no. 1 (2004): 121-128. https://doi.org/10.1016/j.mechrescom.2003.09.004

[11] Sharma, Kushal. "Rheological effects on boundary layer flow of ferrofluid with forced convective heat transfer over an infinite rotating disk." *Pramana* 95, no. 3 (2021): 113. https://doi.org/10.1007/s12043-021-02136-7

[12] Sarkar, Suman, and Bikash Sahoo. "Oblique stagnation flow towards a rotating disc." *European Journal of Mechanics-B/Fluids* 85 (2021): 82-89. https://doi.org/10.1016/j.euromechflu.2020.08.009

[13] Farooq, Umar, Ali Hassan, Nahid Fatima, Muhammad Imran, M. S. Alqurashi, Sobia Noreen, Ali Akgül, and Abdul Bariq. "A computational fluid dynamics analysis on Fe3O4–H2O based nanofluid axisymmetric flow over a rotating disk with heat transfer enhancement." *Scientific Reports* 13, no. 1 (2023): 4679. https://doi.org/10.1038/s41598-023-31734-1

[14] Ming, Chunying, Kexin Liu, Kelu Han, and Xinhui Si. "Heat transfer analysis of Carreau fluid over a rotating disk with generalized thermal conductivity." *Computers & Mathematics with Applications* 144 (2023): 141-149. https://doi.org/10.1016/j.camwa.2023.05.029

[15] Gholinia, M., Kh Hosseinzadeh, H. Mehrzadi, D. D. Ganji, and A. A. Ranjbar. "Investigation of MHD Eyring–Powell fluid flow over a rotating disk under effect of homogeneous–heterogeneous reactions." *Case Studies in Thermal Engineering* 13 (2019): 100356. https://doi.org/10.1016/j.csite.2018.11.007

[16] Doh, Deog-Hee, Gyeong-Rae Cho, E. Ramya, and M. Muthtamilselvan. "Cattaneo-Christov heat flux model for inclined MHD micropolar fluid flow past a non-linearly stretchable rotating disk." *Case Studies in Thermal Engineering* 14 (2019): 100496. https://doi.org/10.1016/j.csite.2019.100496

[17] Sreenivasulu, P., S. R. Gunakala, T. Poornima, N. Bhaskar Reddy, and V. M. Job. "Aligned magnetic field and Navier slip effects on free convective radiative flow of nanofluids with imbedded carbon nanotubes: a Lie group analysis." *SN Applied Sciences* 2, no. 7 (2020): 1283. https://doi.org/10.1007/s42452-020-3105-5

[18] Sreenivasulu, P., S. R. Gunakala, T. Poornima, N. Bhaskar Reddy, and V. M. Job. "Aligned magnetic field and Navier slip effects on free convective radiative flow of nanofluids with imbedded carbon nanotubes: a Lie group analysis." *SN Applied Sciences* 2, no. 7 (2020): 1283. https://doi.org/10.1007/s42452-020-3105-5

[19] Swain, K., M. Mishra, and P. K. Rout. "Magnetohydrodynamics flow of nanofluid past an elongating sheet with exponential space-based heat source and homogeneous-heterogeneous chemical reactions." *Int J Thermofluid Sci Technol* 8 (2021).

[20] Mishra, Swetapadma, Renuprava Dalai, and Kharabela Swain. "Effects of copper and titania nanoparticles on MHD 3D rotational flow over an elongating sheet with convective thermal boundary condition." *International Journal of Ambient Energy* 44, no. 1 (2023): 381-389. https://doi.org/10.1080/01430750.2022.2127892

[21] Mahmud, K., Faisal Z. Duraihem, R. Mehmood, S. Sarkar, and S. Saleem. "Heat transport in inclined flow towards a rotating disk under MHD." *Scientific Reports* 13, no. 1 (2023): 5949. https://doi.org/10.1038/s41598-023-32828-6
[22] Kumar, S. Abhilash Anand, and S. Md Ibrahim. "Cubic B-splines method for Hall and ion slip impacts on unsteady MHD rotating flow past a vertical moving porous plate." *Heat Transfer* 51, no. 4 (2022): 3620-3635. https://doi.org/10.1002/htj.22467
[23] Sharma, Ram Prakash, S. M. Ibrahim, Madhu Jain, and S. R. Mishra. "Chemical reaction effect on MHD rotating fluid over a vertical plate with variable thermal conductivity: A numerical study." *Indian Journal of Pure & Applied Physics (IJPAP)* 56, no. 9 (2018): 732-740.
[24] Mabood, F., S. M. Ibrahim, and G. Lorenzini. "Chemical reaction effects on MHD rotating fluid over a vertical plate embedded in porous medium with heat source." *Journal of Engineering Thermophysics* 26 (2017): 399-415. https://doi.org/10.1134/S1810232817030109
[25] Mabood, F., S. M. Ibrahim, and W. A. Khan. "Framing the features of Brownian motion and thermophoresis on radiative nanofluid flow past a rotating stretching sheet with magnetohydrodynamics." *Results in physics* 6 (2016): 1015-1023. https://doi.org/10.1016/j.rinp.2016.11.046
[26] Zhou, Shuang-Shuang, Muhammad Bilal, Muhammad Altaf Khan, and Taseer Muhammad. "Numerical analysis of thermal radiative maxwell nanofluid flow over-stretching porous rotating disk." *Micromachines* 12, no. 5 (2021): 540. https://doi.org/10.3390/mi12050540
[27] Hussain, Azad, Mohamed Abdelghany Elkotb, Mubashar Arshad, Aysha Rehman, Kottakkaran Sooppy Nisar, Ali Hassan, and C. Ahamed Saleel. "Computational investigation of the combined impact of nonlinear radiation and magnetic field on three-dimensional rotational nanofluid flow across a stretchy surface." *Processes* 9, no. 8 (2021): 1453. https://doi.org/10.3390/pr9081453
[28] Bashir, Muhammad Nauman, Amar Rauf, Sabir Ali Shehzad, Mohsin Ali, and Tahir Mushtaq. "Thermophoresis phenomenon in radiative flow about vertical movement of a rotating disk in porous region." *Advances in Mechanical Engineering* 14, no. 7 (2022): 16878132221115019. https://doi.org/10.1177/16878132221115019
[29] Sharma, Kushal. "FHD flow and heat transfer over a porous rotating disk accounting for Coriolis force along with viscous dissipation and thermal radiation." *Heat Transfer* 51, no. 5 (2022): 4377-4392. https://doi.org/10.1002/htj.22504
[30] Noreen, Sobia, Umar Farooq, Hassan Waqas, Nahid Fatima, M. S. Alqurashi, Muhammad Imran, Ali Akgül, and Abdul Bariq. "Comparative study of ternary hybrid nanofluids with role of thermal radiation and Cattaneo-Christov heat flux between double rotating disks." *Scientific Reports* 13, no. 1 (2023): 7795. https://doi.org/10.1038/s41598-023-34783-8
[31] Arif, Muhammad, Showkat Ahmad Lone, Anwar Saeed, Poom Kumam, Wiboonsak Watthayu, and Ahmed M. Galal. "Thermal analysis of viscoelastic radiative flow of tri-hybrid nanofluid over a rotating disk using different shaped nanoparticles with applications." *ZAMM-Journal of Applied Mathematics and Mechanics/Zeitschrift für Angewandte Mathematik und Mechanik* 103, no. 9 (2023): e202200182. https://doi.org/10.1002/zamm.202200182
[32] Swain, K., S. Mohammed Ibrahim, G. Dharmaiah, and S. Noeiaghdam. "Numerical study of nanoparticles aggregation on radiative 3D flow of maxwell fluid over a permeable stretching surface with thermal radiation and heat source/sink." *Results in Engineering* 19 (2023): 101208. https://doi.org/10.1016/j.rineng.2023.101208
[33] Nagalakshmi, P. S. S., N. Vijaya, and Shaik Mohammed Ibrahim. "Entropy Generation of Three-Dimensional Williamson Nanofluid Flow Explored with Hybrid Carbon Nanotubes over a Stretching Sheet." *CFD Letters* 15, no. 7 (2023): 112-130. https://doi.org/10.37934/cfdl.15.7.112130
[34] Chaudhary, M. A., and J. H. Merkin. "A simple isothermal model for homogeneous-heterogeneous reactions in boundary-layer flow. I Equal diffusivities." *Fluid dynamics research* 16, no. 6 (1995): 311-333. https://doi.org/10.1016/0169-5983(95)00015-6
[35] R. Nandkeolyar, B. K. Mahatha, G. K. Mahato, P. Sibanda, Effect of Chemical Reaction and Heat Absorption on MHD Nanoliquid Flow Past a Stretching Sheet in the Presence of a Transverse Magnetic Field, Magnetochemistry 2018, 4, 18, doi:10.3390/magnetochemistry4010018. https://doi.org/10.3390/magnetochemistry4010018
[36] Renuka, A., M. Muthtamilselvan, Deog-Hee Doh, and Gyeong-Rae Cho. "Effects of homogeneous-heterogeneous reactions in flow of nanofluid between two stretchable rotating disks." *The European Physical Journal Special Topics* 228 (2019): 2661-2676. https://doi.org/10.1140/epjst/e2019-900017-1
[37] Al-Kouz, Wael, Kharabela Swain, Basavarajappa Mahanthesh, and Wasim Jamshed. "Significance of exponential space-based heat source and inclined magnetic field on heat transfer of hybrid nanoliquid with homogeneous–heterogeneous chemical reactions." *Heat Transfer* 50, no. 4 (2021): 4086-4102. https://doi.org/10.1002/htj.22065
[38] Sadiq, M. Adil, and T. Hayat. "Entropy optimized flow of Reiner-Rivlin nanofluid with chemical reaction subject to stretchable rotating disk." *Alexandria Engineering Journal* 61, no. 5 (2022): 3501-3510. https://doi.org/10.1016/j.aej.2021.08.069

[39] Kumar, Sanjay, and Kushal Sharma. "Impacts of Stefan blowing on Reiner–Rivlin fluid flow over moving rotating disk with chemical reaction." *Arabian Journal for Science and Engineering* 48, no. 3 (2023): 2737-2746. https://doi.org/10.1007/s13369-022-07008-9

[40] Gudekote, Manjunatha, and Rajashekhar Choudhari. "Slip effects on peristaltic transport of Casson fluid in an inclined elastic tube with porous walls." *Journal of Advanced Research in Fluid Mechanics and Thermal Sciences* 43, no. 1 (2018): 67-80.

[41] Hamrelaine, Salim, Fateh Mebarek-Oudina, and Mohamed Rafik Sari. "Analysis of MHD Jeffery Hamel flow with suction/injection by homotopy analysis method." *Journal of Advanced Research in Fluid Mechanics and Thermal Sciences* 58, no. 2 (2019): 173-186.

[42] Bakar, Shahirah Abu, Norihan Md Arifin, and Ioan Pop. "Stability analysis on mixed convection nanofluid flow in a permeable porous medium with radiation and internal heat generation." *Journal of Advanced Research in Micro and Nano Engineering* 13, no. 1 (2023): 1-17. https://doi.org/10.37934/armne.13.1.117

[43] Sunitha, Cheela, Prathi Vijaya Kumar, Giulio Lorenzini, and Shaik Mohammed Ibrahim. "A study of thermally radiant williamson nanofluid over an exponentially elongating sheet with chemical reaction via homotopy analysis method." *CFD Letters* 14, no. 5 (2022): 68-86. https://doi.org/10.37934/cfdl.14.5.6886

[44] Roja, P., T. Sankar Reddy, S. M. Ibrahim, Giulio Lorenzini, and Nor Azwadi Che Sidik. "The Effect of thermophoresis on MHD stream of a micropolar liquid through a porous medium with variable heat and mass flux and thermal radiation." *CFD Letters* 14, no. 4 (2022): 118-136. https://doi.org/10.37934/cfdl.14.4.118136

[45] Elfaghi, Abdulhafid MA, Alhadi A. Abosbaia, Munir FA Alkbir, and Abdoulhdi AB Omran. "CFD Simulation of Forced Convection Heat Transfer Enhancement in Pipe Using Al2O3/Water Nanofluid." *Journal of Advanced Research in Micro and Nano Engineering* 7, no. 1 (2022): 8-13. https://doi.org/10.37934/cfdl.14.9.118124

[46] Tripathi, Manoj Kumar, and Aadil Hashim Saifi. "Marangoni Convection in Liquid Bridges due to a Heater/Cooler Ring." *Journal of Advanced Research in Numerical Heat Transfer* 12, no. 1 (2023): 18-25.